Int J Clin Exp Med 2020;13(2):440-449
www.ijcem.com /ISSN:1940-5901/IJCEM0102429

Original Article

Niclosamide ethanolamine prevents muscle wasting by inhibiting p38 MAPK-FoxO3a activation in mice exposed to doxorubicin

Hongyue Zhan[1,3*], Menghua Wang[1*], Pengxun Han[1], Xuewen Yu[2], Yao Wang[1], Wenci Weng[1], Changjian Yuan[1], Yuyan Li[1], Taifen Wang[1], Mumin Shao[2], Huili Sun[1]

Departments of [1]Nephrology, [2]Pathology, Shenzhen Traditional Chinese Medicine Hospital, The Fourth Clinical Medical College of Guangzhou University of Chinese Medicine, Shenzhen, Guangdong, China; [3]Department of Critical Care Medicine, Shantou Hospital of Traditional Chinese Medicine, Shantou, Guangdong, China. [*]Equal contributors.

Received September 17, 2019; Accepted December 11, 2019; Epub February 15, 2020; Published February 28, 2020

Abstract: Introduction: Doxorubicin-induced skeletal muscle wasting is common clinically, and its side effect seems to be associated with patient prognosis. Approaches to preventing skeletal muscle wasting are currently limited. Niclosamide ethanolamine (NEN) can restore body weight and can counteract the side effects of doxorubicin on the kidneys. However, the protective effects of NEN on skeletal muscle have not been investigated. The purpose of the present study was to investigate the protective effects of NEN on the muscles of mice exposed to doxorubicin and their underlying mechanisms. Materials and methods: Male BALB/c mice were used to induce an animal model through a single intravenous injection of doxorubicin and then the mice were randomly assigned to a control (CTRL) group, a doxorubicin group, and a doxorubicin+NEN group. Mice from the doxorubicin+NEN group were fed regular chow supplemented with 2 g/kg NEN in their diet. After two weeks of treatment, muscle strength, running ability, muscle weight, fiber cross-sectional area, fiber type distribution, and the ultrastructure of the muscles were evaluated to verify the protective effects of NEN. Results: With two weeks of treatment, our experiment found that NEN strengthened the muscle force and improved the mice's running endurance. It increased the mass of TA, EDL, and GAs muscle significantly. NEN also alleviated the muscle morphological alterations. It restored the fiber cross-sectional area and thickened the Z-lines of sarcomere. NEN might shift the fibers from type II to type I which might increase mitochondria biogenesis. Moreover, NEN inhibited the p38 mitogen-activated protein kinases (p38 MAPK) and forkhead class O 3a (FoxO3a) activation in the muscles of mice exposed to doxorubicin. Conclusion: This study provides initial evidence that NEN protects the muscles of mice exposed to doxorubicin. The mechanisms might be associated with its inhibition of p38 MAPK-FoxO3a activation.

Keywords: Niclosamide ethanolamine salt, muscle wasting, doxorubicin, p38 MAPK, FoxO3a

Introduction

Doxorubicin, an anthracycline chemotherapeutic drug, has been used to treat a variety of cancers. The side effects of its administration are also common and thus have limited its applications. Skeletal muscle wasting is one of its prominent side effects, which is a devastating condition resulting in a reduction of the quality of life and in high mortality [1]. The prevention of skeletal muscle wasting might have the benefit of promoting patients' prognosis [2]. However, drugs that arrest muscle wasting are few.

Niclosamide is a classic anthelmintic drug widely used to treat parasitic infection. NEN is a salt form of niclosamide, applied to treat many types of diseases including type 1 [3] and type 2 diabetes [4], cancers [5], and renal diseases [6] etc. Importantly, our previous study demonstrated that NEN had the renal protective effect in doxorubicin-induced kidney disease mice [7], an indication that NEN might counteract the side effects of doxorubicin. However, the effects of NEN on muscle wasting have not been elucidated. Interestingly, our recent study found that NEN can restore the body weight of streptozocin (STZ)-induced diabetic mice [3] and the

weight of the skeletal muscles [Unpublished data]. Muscle mass and fatty tissue are the most important factors contributing to total body weight [8]. Accordingly, we proposed that NEN might prevent muscle wasting induced by doxorubicin.

Mechanisms of muscle wasting induced by doxorubicin are greatly complex. A growing body of evidence has demonstrated that the activation of MAPKs is detected in the wasted muscle tissue or cells induced by doxorubicin in vivo and in vitro [9, 10]. Fox03a, as a transcriptional factor, is a downstream of p38 MAPK, and has been proven to be an important molecule relating to muscle atrophy [11, 12]. Moreover, the inhibition of MAPKs and its downstream cascade might prevent muscle wasting induced by chemotherapy [13].

Taking this into account, we aimed to determine the effect of NEN on muscle exposed to doxorubicin and to explore the potential mechanisms.

Materials and methods

Animal model

All the procedures of our animal study were approved by the Guangzhou University of Chinese Medicine Institutional Animal Care and Use Committee and in accordance with the relevant guidelines and regulations. Male BALB/c mice were purchased from the Laboratory Animal Center of Southern Medical University (Guangzhou, China) and were housed in the Central Animal Facility of Shenzhen Graduate School of Peking University at a constant room temperature (20 ± 1°C) under a controlled 12 h light to 12 h dark cycle. Water and food were freely accessible. The experimental mice (weighing 20-25 g) were randomly assigned to three groups: the doxorubicin group (DOX group, n = 6); the doxorubicin+NEN group (DOX+NEN group, n = 6); and the control group (CTRL group, n = 6). Mice from the DOX and the DOX+NEN groups were injected with doxorubicin (10.4 mg/kg, Sigma Aldrich, St. Louis, MO, USA) dissolved in normal saline via the tail vein. The CTRL group mice were injected with an equivalent volume of normal saline. Two weeks after the doxorubicin exposure, chow supplemented with 2 g/kg NEN (2A PharmaChem, Lisle, IL, USA) was used to feed the DOX+NEN group mice. According to our previous study, the suitable dose of NEN supplemented in the diet was determined to be 2 g/kg in this experiment [7]. The CTRL and DOX group mice were fed a regular diet as before. The treatment lasted for two weeks. The mice's body weight was measured every 7 days. The food intake per mouse was measured by determining the home cage food consumption weight every 1-2 weeks.

Grip strength and running test

Grip strength was measured using a dynamometer for mice (ZH-YLS-13A, Anhui Zhenghua Biological Instrument Equipment Co. Ltd., Huaibei, China). Limb grip strength was performed following the previous procedure with a modification [14]. The PC interface software automatically sensed compression or tension and recorded the peak value (in mV). The calibrate factor was measured by using a standard weight (1.98 Newtons). Limb strength (in Newtons) was calculated by peak value (in mV) × calibrate factor. For this assay, three measurements were performed for each mouse and the average of the measurements was used for the analysis.

The running test was done using a treadmill for mice (ZH-PT, Anhui Zhenghua Biological Instrument Equipment Co. Ltd., Huaibei, China). After being acclimated to treadmill running on the day before the experiment, the mice were run on the treadmill for 4-6 min, with the running distance and the times of the electric shocks recorded automatically. The running ability was expressed using electric shocks per mile every second (Shocks/mile/s).

Tissue preparation

The mice were sacrificed two weeks after the NEN treatment (four weeks after doxorubicin injection). The tibialis anterior (TA), the soleus (SOL), the extensor digitorum longus (EDL), and the gastrocnemius (GAs) were dissected and weighed. The TA muscle tissues were fixed in 10% formalin and then stained with PAS for the histopathological examination. The EDL muscle tissue (1 mm^3) was fixed in 2.5% glutaraldehyde and then post-fixed in 1% osmic acid for examination using a transmission electron microscope (TEM, JEM-1400, JEOL, Tokyo, Japan). The GAs muscle tissues were immediately snap-frozen in liquid nitrogen and stored at -80°C for later analysis. The soleus muscles were embedded in O.C.T. compound (Tissue-

Tek, Sakura Finetek, USA), frozen in liquid nitrogen-cooled isopentane, stored at -80°C, and cut into 10 mm thick cryosections with a cryostat (CM1950, Leica, Germany), and then maintained at -20°C for fiber type determination.

Morphological studies

The muscles were photographed using a digital camera. Paraffin sections of the TA muscles were stained with periodic acid-Schiff (PAS) according to the standard protocols. The cross-sectional area was analyzed using ImageJ Software (National Institutes of Health, Bethesda, MD, USA). Longitude section fields were selected for EM analysis.

Fiber type determination

Primary antibodies against MHC-I (BA-F8), MHC-IIa (SC-71) and MHC-IIb (BF-F3) purchased from the Developmental Studies Hybridoma Bank (University of Iowa, National Institutes of Health, USA) and secondary antibodies purchased from Invitrogen (USA) were used to determine the muscle fiber type. Procedures described previously were performed [15]. Individual images were taken across the entire cross-section using a confocal microscope (LSM710, Carl Zeiss, Oberkochen, Germany) and assembled into a composite panoramic image with Photoshop 7.0 (Adobe, USA). All fibers within the entire muscle were characterized, and the fiber counts and fiber type percentages were analyzed.

Immunoblotting analysis

Snap-frozen GAs muscle tissues were homogenized in a lysis buffer and prepared in a sample loading buffer (Bio-Rad, Hercules, CA, USA). Next, the SDS-PAGE protein separation procedures were performed, and the separated proteins were transferred to polyvinylidene difluoride (PVDF) membranes (Merck Millipore, Danvers, MA, USA). The membranes were blocked in TBS containing 5% nonfat dry milk for 1 h at room temperature, then incubated and gently shaken overnight at 4°C with primary antibodies. After washing with TBS, the membranes were incubated with secondary antibodies for 1 h at room temperature with shaking. The protein bands were measured and analyzed using the ChemiDoc™ MP Imaging System (Bio-Rad, Hercules, CA, USA). The results were expressed as the integrated optical density relative to Glyceraldehyde-3-phosphate dehydrogenase (GAPDH), which was used as the loading control. The primary antibodies against p-p38 MAPK, p38 MAPK, p-Erk1/2, Erk1/2, and FoxO3a were purchased from Cell Signaling Technology (Danvers, MA, USA). The primary antibody against GAPDH was obtained from Proteintech Group, Inc. (Chicago, IL, USA).

Statistical analysis

The data were expressed as the means ± SD. Statistical differences between two groups were analyzed using unpaired Student's *t* tests. Differences among multiple groups were analyzed using one-way ANOVA. The statistical analyses were performed using SPSS 16.0 statistical software, and $P < 0.05$ was considered statistically significant.

Results

NEN prevented muscle weakness in mice exposed to doxorubicin

Following the doxorubicin administration, the mice exhibited a decline in limb muscle strength and a rapid increase in fatigue. As shown in **Figure 1**, NEN prevented the doxorubicin induced muscle weakness. The limb grip strengths of the mice in the DOX+NEN treated group were much stronger than those in the DOX group (DOX: 1.57 ± 0.22 N v.s. DOX+NEN: 1.86 ± 0.05 N; $P < 0.05$) (**Figure 1A**). The running test showed that NEN reduced fatigue in mice exposed to doxorubicin as well (DOX: 1.19 ± 0.64 Shocks/m/s v.s. DOX+NEN: 0.37 ± 0.32 Shocks/m/s; $P < 0.05$) (**Figure 1B**).

NEN restored body weight without improving food intake in mice exposed to doxorubicin

The body weight and food intake of the transient mice decreased at day 7 after the doxorubicin exposure. Compared with the DOX group, the body weight of the mice in the DOX+NEN group was much heavier (DOX: 0.939 ± 0.024 fold v.s. DOX+NEN: 1.036 ± 0.054 fold; $P < 0.001$) (**Figure 2A**). The overall food intake started increasing at day 14, and 2 weeks of NEN treatment did not improve it further (**Figure 2B**). Interestingly, the biochemistry parameters of the nutrient state had changed slightly without being statistically significant at the end of the experiment (**Figure 2C-F**).

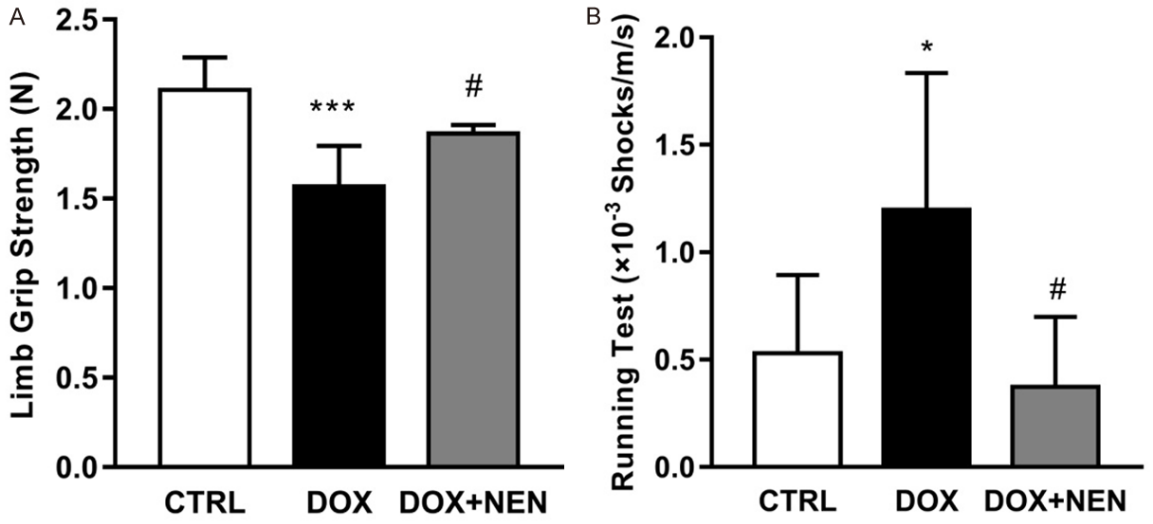

Figure 1. NEN enhanced the muscle force and exercise endurance. A. Limb grip strength. B. Running test. It was expressed by using an electric shock several times every mile per second. n = 6 per group. $^{*}P < 0.05$ and $^{***}P < 0.001$ vs. the CTRL group. $^{\#}P < 0.05$ vs. the DOX group.

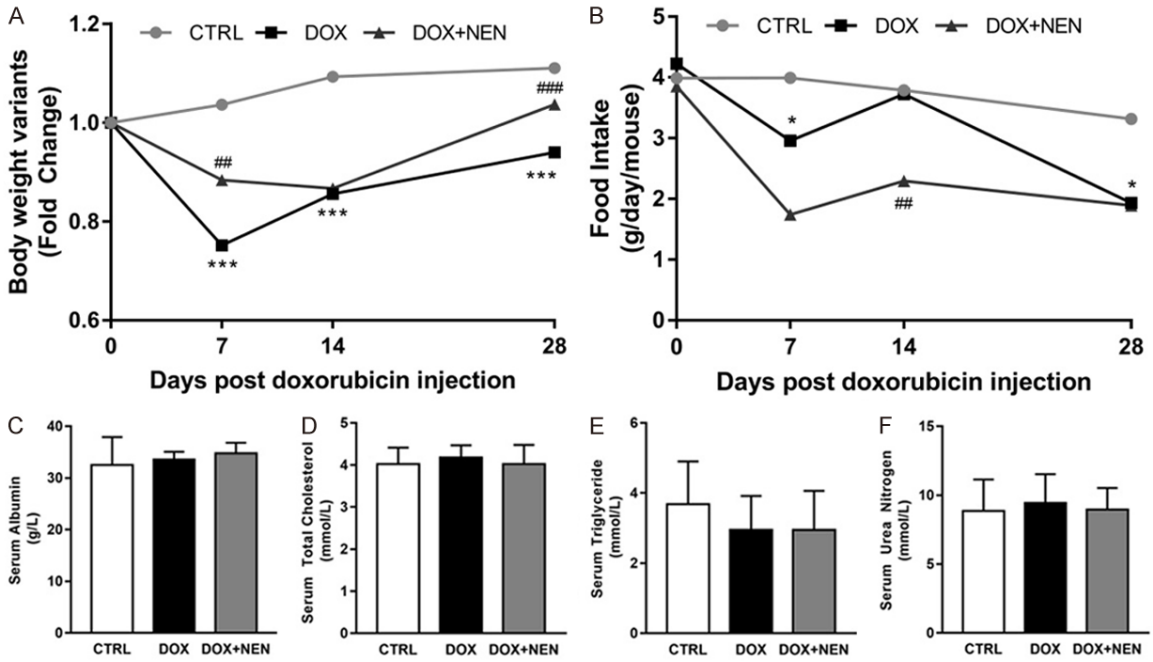

Figure 2. NEN restored the body weight without improving the food intake of mice exposed to doxorubicin (A). Body weight variations vs. day 0 (n = 6 each group) (B). Food intake had no increase after NEN administration (n = 1-3 mice per cage, N = 3-4 cages each group). Biochemistry parameters associated with nutrition, including serum albumin (C), serum total cholesterol (D), serum triglyceride (E) and serum urea nitrogen (F). $^{*}P < 0.05$ and $^{***}P < 0.001$ vs. the CTRL group. $^{\#\#}P < 0.01$ and $^{\#\#\#}P < 0.001$ vs. the DOX group.

NEN counteracted with muscle atrophy of mice exposed to doxorubicin

Doxorubicin resulted in dramatic limb muscle atrophy, but the NEN counteracted it (**Figure 3A**). NEN increased the muscle mass of TA (DOX: 0.035 ± 0.003 g v.s. DOX+NEN: 0.041 ± 0.004 g; P < 0.05) (**Figure 3B**), EDL (DOX: 0.008 ± 0.001 g v.s. DOX+NEN: 0.010 ± 0.001 g; P < 0.05) (**Figure 3C**) and GAs (DOX: 0.105 ± 0.007

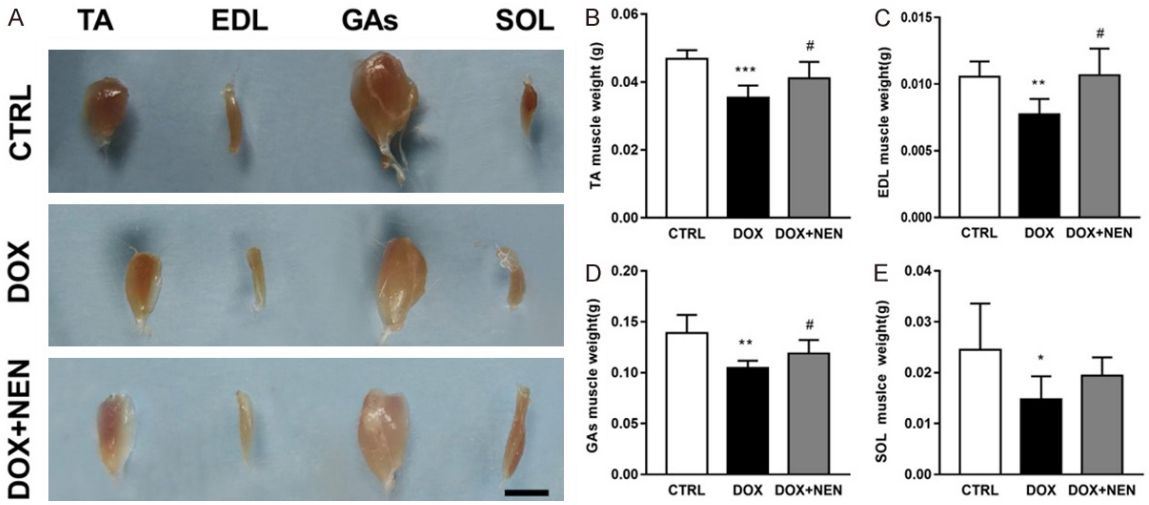

Figure 3. NEN counteracted with muscle atrophy. (A) Representative gross muscle images of each group. Muscle weight of tibialis anterior (B), extensor digitorum longus (C), gastrocnemius (D), soleus (E). n = 6 per group. $^{*}P < 0.05$, $^{**}P < 0.01$ and $^{***}P < 0.001$ vs. the CTRL group. $^{\#}P < 0.05$ vs. the DOX group.

g v.s. DOX+NEN: 0.119 ± 0.013 g; P < 0.05) (**Figure 3D**) significantly but not SOL (DOX: 0.015 ± 0.004 g v.s. DOX+NEN: 0.019 ± 0.003 g; P = 0.078) (**Figure 3E**).

NEN restored the muscle fiber size and muscle ultra-structure of the mice exposed to doxorubicin

To determine the impacts of NEN on the muscle fiber of doxorubicin treated mice, a cross-sectional area of the fibers was measured. Remarkably, the mean cross-sectional area of muscle fiber increased two weeks after the NEN administration (CTRL: 1415.370 ± 179.993 um^2, DOX: 888.660 ± 109.322 um^2 and DOX+NEN: 1191.515 ± 179.338 um^2; n = 5-6) (**Figure 4A**, **4C**). Doxorubicin caused a shift towards more small fibers, and NEN also normalized this change (**Figure 4B**). Likewise, the TEM morphologic assessment of the EDL muscles revealed alternations at the sarcomeric level. The Z-lines in the mice treated with doxorubicin were thinner than the ones in the CTRL group. However, the Z-lines in the NEN group were thicker compared with the DOX group (**Figure 4D**).

NEN changed the distribution of the muscle fiber type

The soleus muscle was used for the fiber type determination. As the figures show, the distribution of muscle fiber type in the CTRL and DOX treated groups were similar (**Figure 5A-C**). But compared with the DOX treated group, a significant change of fiber composition was seen in the DOX+NEN group. After two weeks' of NEN treatment, the type I fiber compositions were 37.222 ± 5.32%, 36.172 ± 3.75% and 41.799 ± 3.52% in the CTRL, DOX and DOX+NEN groups respectively. These showed that the distribution of muscle fiber type of doxorubicin-induced mice shifts from type II to type I were significant.

NEN inhibited the activation of the p38 MAPK/FoxO3a signaling pathway

Western blotting showed that the p38 MAPK and FoxO3a protein levels increased significantly in the DOX treated group, by 1.39-fold and 2.11-fold respectively compared with the CTRL group. Treated with NEN for two weeks, the activation of p38MAPK and FoxO3a were downregulated (**Figure 6A**, **6B**, **6D**). Erk1/2 was also a pro-atrophic marker. In the present study, no substantial change of Erk1/2 was seen in mice treated with DOX group compared with the mice in the other two groups (**Figure 6A**, **6C**).

Discussion

Although intensive efforts have been made to prevent doxorubicin-induced cardiac myocyte injuries [16], approaches that counteract skeletal muscle wasting induced by doxorubicin are

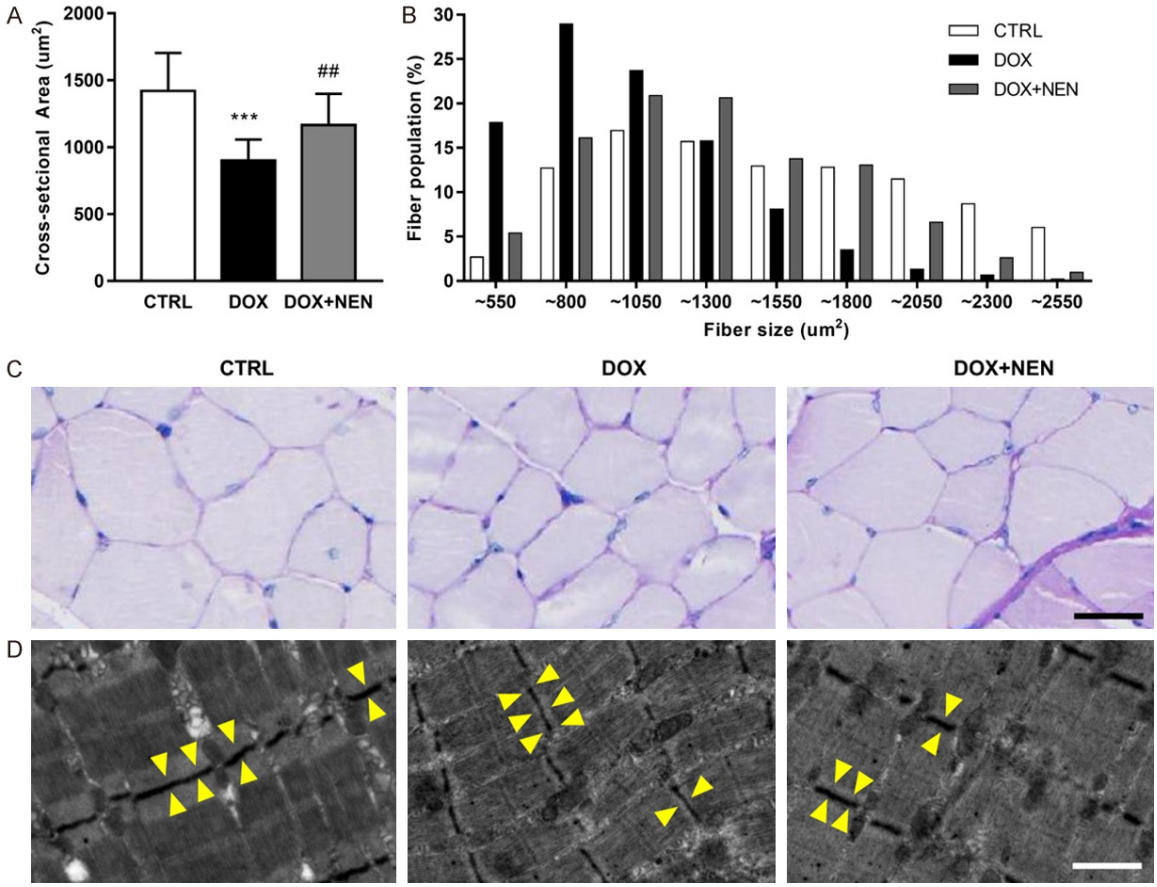

Figure 4. NEN alleviated muscle morphological alterations induced by doxorubicin. Tibialis anterior muscle fiber cross-sectional area (A) and the fiber size distribution (B). (C) Representative images of fiber size alteration (PAS stained. scale bar, 30 um). (D) Representative TEM images of Z-lines (braced with a yellow arrow) of each group (scale bar, 1 um). n = 5-6 per group. $^{***}P < 0.001$ vs. the CTRL group. $^{\#\#}P < 0.01$ vs. the DOX group.

limited. In the present study, our results indicate, for the first time, that NEN prevented the muscle wasting in mice exposed to doxorubicin. Additionally, the underlying mechanisms might be associated with the inhibition of the p38 MAPK/FoxO3a signaling pathway.

Doxorubicin administration commonly causes muscle wasting [17, 18]. Muscle atrophy with reduced muscle masses and TA fiber size were observed, which were consistent with previously reported works [19]. Along with the muscle atrophy, both limb grip strength and running endurance were reduced. Furthermore, for the two-week treatment period, our study demonstrated that NEN restored the muscle masses and morphologic changes as well as shifted the fiber size distribution rightward. Our study also found that NEN enhanced muscle function.

The mechanisms of muscle wasting induced by doxorubicin had not been elucidated clearly. A recent study revealed that it was associated with malnutrition [20]. Consistent with our observations, food intake and body weight were reduced transiently after doxorubicin administration. However, the biochemistry parameters reflecting nutrition, such as serum albumin, serum urea nitrogen, serum total cholesterol, and serum triglyceride, had no significant changes in the present experiment. These findings suggest that doxorubicin induced muscle wasting might be explained by malnutrition partially, and the direct injury effect of certain agents might exist [21]. Interestingly, NEN restored the body weight of mice exposed to doxorubicin without improving their food intake. Thus, we proposed that the underlying mechanism of NEN counteracting the muscle wasting should be explained beyond nutrition improvement.

It was widely reported that doxorubicin-induced muscle wasting is caused by inflammation,

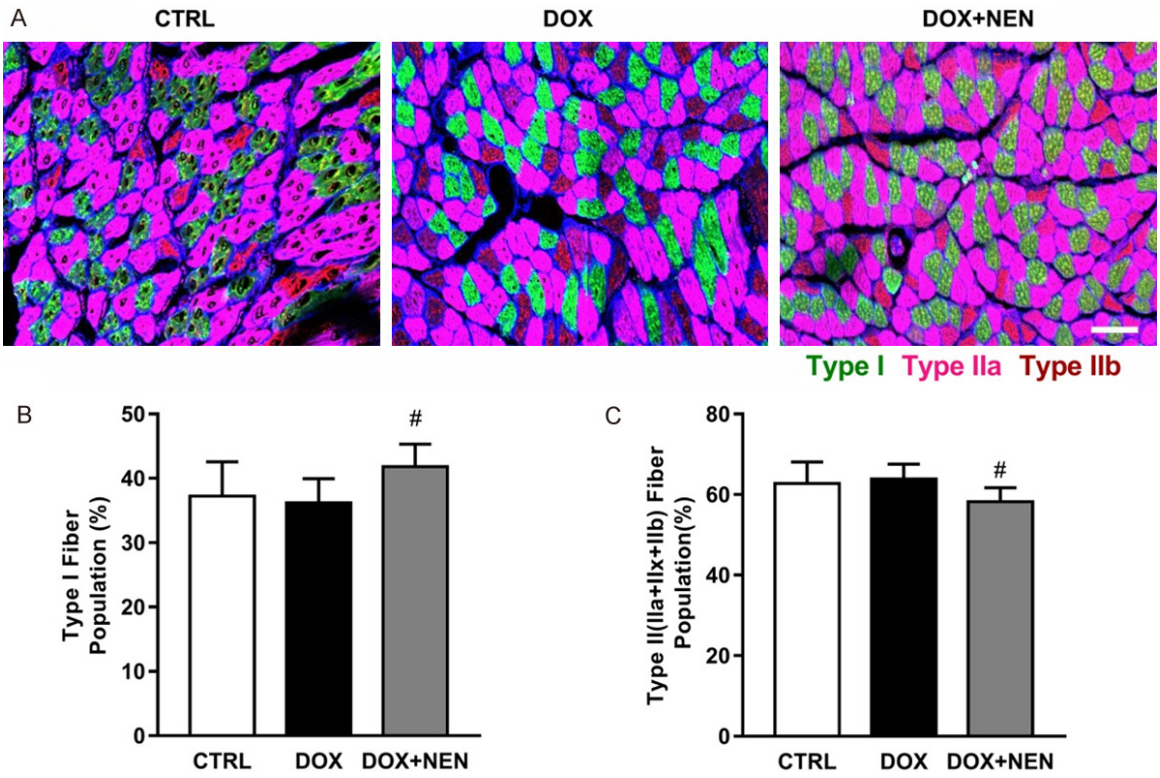

Figure 5. NEN changed the distribution of the muscle fiber type. A. Representative images of the fiber type distribution (Immunofluorescence stained. scale bar, 100 um). Shown are type I (green), type IIa (magenta), type IIb (red), type IIx (unstained) fibers. B, C. Type I and Type II (IIa+IIx+IIb) population. n = 5, for each group. $^{\#}P < 0.05$ vs. the DOX group.

apoptosis, proteolysis, or oxidative stress [22, 23] directly. P38 MAPK and extracellular regulated protein kinases 1/2 (Erk1/2) are the key regulators of the activities of many transcription factors and enzymes [24], and they have a wide spectrum of biological effects, including pro-inflammation, pro-apoptosis, and inducing oxidative stress. Previous studies [20, 25, 26] demonstrated that both p38 MAPK and Erk1/2 are elevated in atrophic muscle and were proven to be associated with muscle wasting by controlling myocyte survival and proliferation. Interestingly, in our experiment, the p38 MAPK levels were higher in doxorubicin treated mice, but Erk1/2 had no remarkable change. The conflicting results might be due to diversity in species, different chemotherapeutic agents, or the dosage of doxorubicin. FoxO3a, a transcription factor regulating muscle masses, was reported to be over expressed in atrophic skeletal muscle of doxorubicin treated mice, a finding which is consistent with the present study [27]. Furthermore, muscle specific FoxO3a expression and transcriptional activity could be regulated by p38 MAPK [26]. More importantly, for the two-weeks long treatment, our findings showed that NEN inhibited the expression of p38 MAPK and downregulated FoxO3a analogously. Altogether, we postulate that the observed attenuation of doxorubicin-induced skeletal muscle wasting by NEN was associated with the p38 MAPK/FoxO3a signaling pathway.

Additionally, in this study, we observed that NEN promoted the percentage of type I fibers in soleus muscle, which are rich in mitochondria and use predominantly oxidative phosphorylation for energy production. Mitochondria depletion seems to be associated with chemotherapeutic-induced muscle wasting [25], and NEN has proven to be a safe mitochondria uncoupler [28]. Therefore, we think that the effects of NEN on muscle wasting might be associated with the increasing mitochondria biogenesis.

In summary, the evidence presented here shows that NEN can prevent muscle wasting and alleviate the morphologic and functional

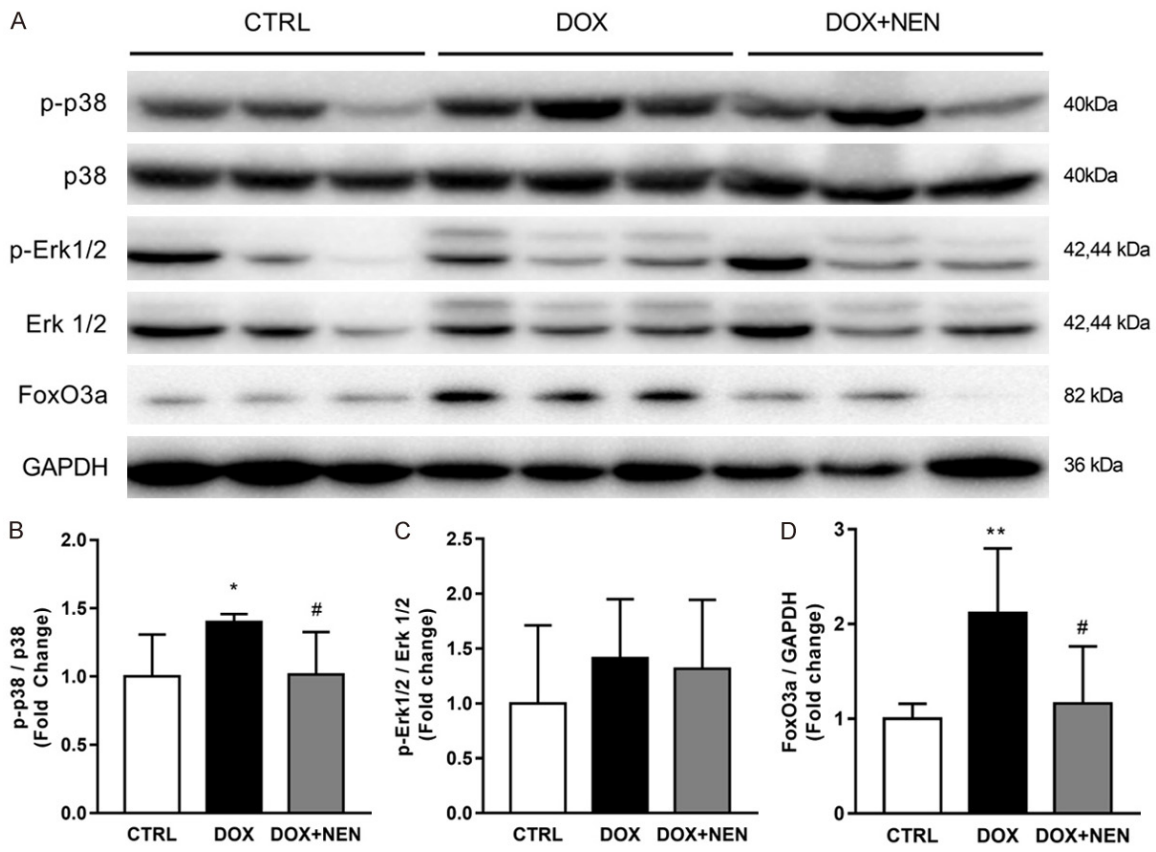

Figure 6. NEN inhibited p38 MAPK and FoxO3a activation in the doxorubicin induced wasting muscle. A. Western blot images of p38 MAPK, FoxO3a, and Erk1/2 in the GAs muscle tissue of various groups. B, C. Bar graphs showing the fold change of p-p38, p-Erk1/2 expression after the normalization to the total p38 and total Erk1/2 expression respectively. D. Bar graphs showing the fold change of FoxO3a expression after normalization to the GAPDH. n = 6 for each group. $^{*}P < 0.05$ and $^{**}P < 0.01$ vs. the CTRL group. $^{\#}P < 0.05$ vs. the DOX group.

alterations of mice exposed to doxorubicin. The mechanisms might be associated with the inhibition of p38 MAPK-FoxO3a activation.

Acknowledgements

This study was supported by grants from the National Natural Science Foundation of China (81673794, 81202818), the Shenzhen Science and Technology Project (JCYJ2016033-0171116798), and the Sanming Project of Medicine in Shenzhen (SZSM201512040).

Disclosure of conflict of interest

None.

Address correspondence to: Huili Sun, Department of Nephrology, Shenzhen Traditional Chinese Medicine Hospital, The Fourth Clinical Medical College of Guangzhou University of Chinese Medicine, 1 Fuhua Road, Futian District, Shenzhen 518033, Guangdong, China. Tel: +86-755-83214509; Fax: +86-755-88356033; E-mail: sunhuili2011@126.com; Mumin Shao, Department of Pathology, Shenzhen Traditional Chinese Medicine Hospital, The Fourth Clinical Medical College of Guangzhou University of Chinese Medicine, 1 Fuhua Road, Futian District, Shenzhen 518033, Guangdong, China. Tel: +86-755-23987273; Fax: +86-755-88356033; E-mail: smm026@163.com

References

[1] Elsea CR, Kneiss JA and Wood LJ. Induction of IL-6 by cytotoxic chemotherapy is associated with loss of lean body and fat mass in tumor-free female mice. Biol Res Nurs 2015; 17: 549-557.

[2] Pin F, Couch ME and Bonetto A. Preservation of muscle mass as a strategy to reduce the toxic effects of cancer chemotherapy on body composition. Curr Opin Support Palliat Care 2018; 12: 420-426.

[3] Han P, Shao M, Guo L, Wang W, Song G, Yu X, Zhang C, Ge N, Yi T, Li S, Du H and Sun H. Niclosamide ethanolamine improves diabetes and diabetic kidney disease in mice. Am J Transl Res 2018; 10: 1071-1084.
[4] Guo J, Tao H, Alasadi A, Huang Q and Jin S. Niclosamide piperazine prevents high-fat diet-induced obesity and diabetic symptoms in mice. Eat Weight Disord 2017; 24: 91-96.
[5] Alasadi A, Chen M, Swapna GVT, Tao H, Guo J, Collantes J, Fadhil N, Montelione GT and Jin S. Effect of mitochondrial uncouplers niclosamide ethanolamine (NEN) and oxyclozanide on hepatic metastasis of colon cancer. Cell Death Dis 2018; 9: 215.
[6] Han P, Zhan H, Shao M, Wang W, Song G, Yu X, Zhang C, Ge N, Yi T, Li S and Sun H. Niclosamide ethanolamine improves kidney injury in db/db mice. Diabetes Res Clin Pract 2018; 144: 25-33.
[7] Han P, Yuan C, Wang Y, Wang M, Weng W, Zhan H, Yu X, Wang T, Li Y, Yi W, Shao M, Li S, Yi T and Sun H. Niclosamide ethanolamine protects kidney in adriamycin nephropathy by regulating mitochondrial redox balance. Am J Transl Res 2019; 11: 855-864.
[8] Lancaster GI and Henstridge DC. Body composition and metabolic caging analysis in high fat fed mice. J Vis Exp 2018.
[9] Ruan Y, Dong C, Patel J, Duan C, Wang X, Wu X, Cao Y, Pu L, Lu D, Shen T and Li J. SIRT1 suppresses doxorubicin-induced cardiotoxicity by regulating the oxidative stress and p38MAPK pathways. Cell Physiol Biochem 2015; 35: 1116-1124.
[10] Hydock DS, Lien CY, Jensen BT, Schneider CM and Hayward R. Characterization of the effect of in vivo doxorubicin treatment on skeletal muscle function in the rat. Anticancer Res 2011; 31: 2023-2028.
[11] Al-Nassan S and Fujino H. Exercise preconditioning attenuates atrophic mediators and preserves muscle mass in acute sepsis. Gen Physiol Biophys 2018; 37: 433-441.
[12] Reed SA, Sandesara PB, Senf SM and Judge AR. Inhibition of FoxO transcriptional activity prevents muscle fiber atrophy during cachexia and induces hypertrophy. FASEB J 2012; 26: 987-1000.
[13] Hulmi JJ, Nissinen TA, Rasanen M, Degerman J, Lautaoja JH, Hemanthakumar KA, Backman JT, Ritvos O, Silvennoinen M and Kivela R. Prevention of chemotherapy-induced cachexia by ACVR2B ligand blocking has different effects on heart and skeletal muscle. J Cachexia Sarcopenia Muscle 2018; 9: 417-432.
[14] Bonetto A, Andersson DC and Waning DL. Assessment of muscle mass and strength in mice. Bonekey Rep 2015; 4: 732.
[15] Bloemberg D and Quadrilatero J. Rapid determination of myosin heavy chain expression in rat, mouse, and human skeletal muscle using multicolor immunofluorescence analysis. PLoS One 2012; 7: e35273.
[16] Cao Y, Ruan Y, Shen T, Huang X, Li M, Yu W, Zhu Y, Man Y, Wang S and Li J. Astragalus polysaccharide suppresses doxorubicin-induced cardiotoxicity by regulating the PI3k/Akt and p38MAPK pathways. Oxid Med Cell Longev 2014; 2014: 674219.
[17] Gilliam LA and St Clair DK. Chemotherapy-induced weakness and fatigue in skeletal muscle: the role of oxidative stress. Antioxid Redox Signal 2011; 15: 2543-2563.
[18] Gouspillou G, Scheede-Bergdahl C, Spendiff S, Vuda M, Meehan B, Mlynarski H, Archer-Lahlou E, Sgarioto N, Purves-Smith FM, Konokhova Y, Rak J, Chevalier S, Taivassalo T, Hepple RT and Jagoe RT. Anthracycline-containing chemotherapy causes long-term impairment of mitochondrial respiration and increased reactive oxygen species release in skeletal muscle. Sci Rep 2015; 5: 8717.
[19] Gilliam LAA, Fisher-Wellman KH, Lin CT, Maples JM, Cathey BL and Neufer PD. The anticancer agent doxorubicin disrupts mitochondrial energy metabolism and redox balance in skeletal muscle. Free Radic Biol Med 2013; 65: 988-996.
[20] Nissinen TA, Degerman J, Räsänen M, Poikonen AR, Koskinen S, Mervaala E, Pasternack A, Ritvos O, Kivelä R and Hulmi JJ. Systemic blockade of ACVR2B ligands prevents chemotherapy-induced muscle wasting by restoring muscle protein synthesis without affecting oxidative capacity or atrogenes. Sci Rep 2016; 6: 32695.
[21] Hayward R, Hydock D, Gibson N, Greufe S, Bredahl E and Parry T. Tissue retention of doxorubicin and its effects on cardiac, smooth, and skeletal muscle function. J Physiol Biochem 2013; 69: 177-187.
[22] Elsea CR, Roberts DA, Druker BJ and Wood LJ. Inhibition of p38 MAPK suppresses inflammatory cytokine induction by etoposide, 5-fluorouracil, and doxorubicin without affecting tumoricidal activity. PLoS One 2008; 3: e2355.
[23] Min K, Kwon OS, Smuder AJ, Wiggs MP, Sollanek KJ, Christou DD, Yoo JK, Hwang MH, Szeto HH, Kavazis AN and Powers SK. Increased mitochondrial emission of reactive oxygen species and calpain activation are required for doxorubicin-induced cardiac and skeletal muscle myopathy. J Physiol 2015; 593: 2017-2036.
[24] Sun Y, Liu WZ, Liu T, Feng X, Yang N and Zhou HF. Signaling pathway of MAPK/ERK in cell proliferation, differentiation, migration, senes-

cence and apoptosis. J Recept Signal Transduct Res 2015; 35: 600-604.
[25] Barreto R, Waning DL, Gao H, Liu Y, Zimmers TA and Bonetto A. Chemotherapy-related cachexia is associated with mitochondrial depletion and the activation of ERK1/2 and p38 MAPKs. Oncotarget 2016; 7: 43442-43460.
[26] Yoshioka Y, Yamashita Y, Kishida H, Nakagawa K and Ashida H. Licorice flavonoid oil enhances muscle mass in KK-A(y) mice. Life Sci 2018; 205: 91-96.
[27] Kavazis AN, Smuder AJ and Powers SK. Effects of short-term endurance exercise training on acute doxorubicin-induced FoxO transcription in cardiac and skeletal muscle. J Appl Physiol 2014; 117: 223-230.
[28] Tao H, Zhang Y, Zeng X, Shulman GI and Jin S. Niclosamide ethanolamine-induced mild mitochondrial uncoupling improves diabetic symptoms in mice. Nat Med 2014; 20: 1263-1269.